

## Simultaneous Magnetic and Charge Doping of Topological Insulators with Carbon

Lei Shen (沈雷),\* Minggang Zeng, Yunhao Lu, Ming Yang, and Yuan Ping Feng<sup>†</sup>

Department of Physics, 2 Science Drive 3, National University of Singapore, Singapore 117542, Singapore  
(Received 20 March 2013; revised manuscript received 25 May 2013; published 5 December 2013)

A two-step doping process, magnetic followed by charge or vice versa, is required to produce *massive* topological surface states (TSS) in topological insulators for many physics and device applications. Here, we demonstrate simultaneous magnetic and hole doping achieved with a single dopant, carbon, in  $\text{Bi}_2\text{Se}_3$  by first-principles calculations. Carbon substitution for Se ( $\text{C}_{\text{Se}}$ ) results in an opening of a sizable surface Dirac gap (up to 82 meV), while the Fermi level remains inside the bulk gap and close to the Dirac point at moderate doping concentrations. The strong localization of  $2p$  states of  $\text{C}_{\text{Se}}$  favors spontaneous spin polarization via a  $p$ - $p$  interaction and formation of ordered magnetic moments mediated by surface states. Meanwhile, holes are introduced into the system by  $\text{C}_{\text{Se}}$ . This dual function of carbon doping suggests a simple way to realize insulating massive TSS.

DOI: [10.1103/PhysRevLett.111.236803](https://doi.org/10.1103/PhysRevLett.111.236803)

PACS numbers: 73.20.At, 68.35.Dv, 71.15.Mb

The second-generation 3D topological insulators (TIs),  $\text{Bi}_2\text{Se}_3$  and  $\text{Bi}_2\text{Te}_3$ , are a class of time-reversal-invariant materials characterized by an insulating bulk state and a conducting surface state consisting of a Dirac cone [1,2]. Such massless surface states are protected by time-reversal symmetry (TRS) and immune to surface disorders such as vacancies [3,4]. Many striking physics and device applications of TIs have been proposed, such as the quantum anomalous Hall effect (QAHE) [5,6], magnetic monopole imaging [7], topological contribution to Faraday and Kerr effects [8], and TI-based  $p$ - $n$  junctions [9]. To enable the above applications, it is necessary to open a surface energy gap as well as keep the Fermi level ( $E_f$ ) inside the bulk gap [8]. It is proposed that doping TIs by magnetic transition metals (TMs), such as Fe and Mn, could break the TRS and open a surface gap [3], which has been the most common experimental approach [5,6,10–17]. Recently, it has been demonstrated that the magnetic proximity effect, induced by a covered magnetic insulator (MnSe, EuS), can be used to open a small Dirac gap in  $\text{Bi}_2\text{Se}_3$ , due to the overlapping of topological and ordinary interfacial states [18,19]. However, in these experiments, the existence of anionic vacancies in the as-grown  $\text{Bi}_2\text{Se}_3$  thin films leads to a typical  $n$ -type material [10,11,20]. To bring the  $E_f$  inside the bulk gap from the bulk conduction band, the excess electrons must be compensated (via hole doping), which can be achieved by doping with divalent cations ( $\text{Mg}^{2+}$  or  $\text{Ca}^{2+}$ ) [10] or chemical molecules with strong electron-accepting ability ( $\text{NO}_2$ , CO) [11,20,21]. Nevertheless, it remains a challenge to find a reliable yet simple scenario to produce out-of-plane magnetization, a stable long-range magnetic order, and proximity of  $E_f$  to the Dirac point. These three conditions are necessary in order to experimentally observe the Dirac gap and/or QAHE by using the approach of magnetic doping [3,6,22–25].

The spontaneous spin polarization and local moments in carbon-doped ZnO, a diluted magnetic semiconductor

(DMS), has been successfully demonstrated both experimentally and theoretically [26,27]. Since O and Se have similar electronic configurations and chemical properties, and C has a quite similar electronegativity (2.55) but two more valence holes compared to Se, one can expect that substitution of C for Se would compensate both Se vacancies and excess electrons in the as-grown  $\text{Bi}_2\text{Se}_3$ . This motivated us to consider carbon doping as a means to achieve massive topological surface states (TSS) in  $\text{Bi}_2\text{Se}_3$ .

In this Letter, we report results of our first-principles investigation on TSS of carbon-doped  $\text{Bi}_2\text{Se}_3$ . The computational details are given in the Supplemental Material [28]. It is found that substitution of C for Se in  $\text{Bi}_2\text{Se}_3$  introduces local moments as well as holes. Carbon doping can lead to simultaneous opening of the Dirac gap up to 82 meV and pinning of  $E_f$  inside the bulk energy gap. It is striking that magnetic doping and ordering can be achieved by using a nonmagnetic dopant (C). We discuss the origin of the magnetic moment, the mechanism of magnetic coupling, and the cause of magnetocrystalline anisotropy in a carbon-doped TI system and compare them with TM-doped TIs. The effects of the carrier density and impurity concentration on the electronic structure are also discussed.

We first consider an ideal  $\text{Bi}_2\text{Se}_3$  surface. Figure 1(a) shows the band structure calculated by using a  $3 \times 3$  slab supercell 7 quintuple layers (QLs) thick with the ideal  $\text{Bi}_2\text{Se}_3$  surface. As can be seen, the  $\Gamma$  Dirac point and the Fermi level ( $E_f$ ) are just above the bulk valence band (BVB). However, the experimentally observed  $E_f$  of undoped  $\text{Bi}_2\text{Se}_3$  is often near the bulk conduction band (BCB) and could be as far as 300 meV away from the Dirac point [6,10,11,20,29]. This is due to Se vacancies, which are easily formed in experimental conditions (Bi rich), leading to a typical  $n$ -type doping of  $\text{Bi}_2\text{Se}_3$  [6,10,11,20,29]. First-principles calculations have confirmed this  $n$ -type doping in  $\text{Bi}_2\text{Se}_3$  with Se vacancies [21] (see the Supplemental Material [28]).

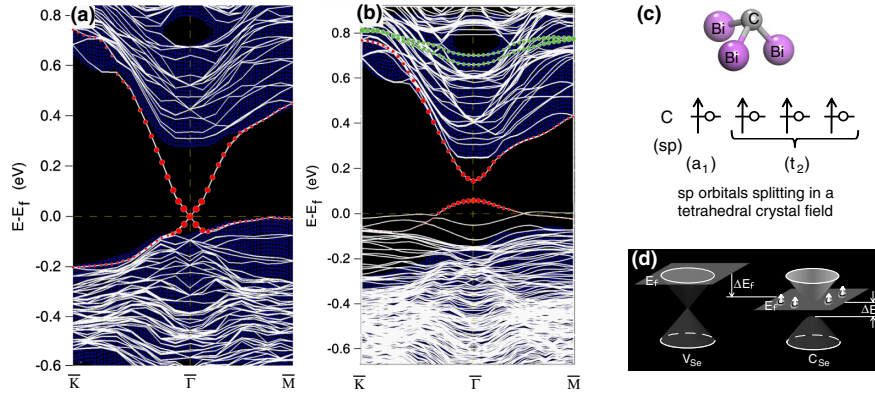


FIG. 1 (color online). Calculated band structure of  $\text{Bi}_2\text{Se}_3$  without a defect (a) and with substitutional carbon doping in the surface layer (b). The topological surface states and carbon impurity states are mainly located in the energy range 0–0.2 eV and 0.7–0.8 eV, indicated by red and green, respectively. The weight of states in each band is shown by the circle size. The bulk band is projected onto the two-dimensional Brillouin zone (blue). (c) Schematic diagram of carbon substitutional doping on the outermost surface layer and its orbital splitting. (d) The schematic illustration of band structures of as-grown  $\text{Bi}_2\text{Se}_3$  (with Se vacancies) and C-doped  $\text{Bi}_2\text{Se}_3$ , respectively. All band structures are calculated by using a symmetric  $3 \times 3$  slab supercell with 7 QLs of  $\text{Bi}_2\text{Se}_3$ . The top and bottom surfaces are identical, and each contains two  $\text{C}_{\text{Se}}$ .

We next consider substitutional carbon doping at a selenium site on the outermost surface layer of  $\text{Bi}_2\text{Se}_3$ , which can be regarded as a filling of surface Se vacancies by carbon. Theoretically, it should not be difficult to fill the Se vacancy in  $\text{Bi}_2\text{Se}_3$  with carbon. This is because carbon has the same electronegativity (2.55) as Se but a much smaller atomic radius (70 pm). Moreover, the large interstitial space in the  $\text{Bi}_2\text{Se}_3$  crystal lattice, due to the large covalent radius of Bi (146) and Se (116), is able to facilitate diffusion of carbon to  $\text{V}_{\text{Se}}$  sites on the  $\text{Bi}_2\text{Se}_3$  surface. As the doping concentration increases, carbon can further replace other selenium atoms during high-temperature annealing [13]. Here we consider a  $\text{C}_{\text{Se}}$  in the outmost layer. Even though the outermost Se layer is less energetically favored for substitutional carbon doping, which has a formation energy of 52 meV higher than that in the third Se layer [in the first QL but on the van der Waals' (vdW) gap side], based on our formation energy calculation,  $\text{C}_{\text{Se}}$  can be expected to be rich in the outermost Se layer, since experimentally doping is typically done through diffusion of dopants into grown  $\text{Bi}_2\text{Se}_3$  samples [10,11,13]. Furthermore, surface doping results in a more direct effect on the topological surface states. The calculated band structure of  $\text{Bi}_2\text{Se}_3$  with carbon substitutional doping is shown in Fig. 1(b). It shows that carbon doping leads to the opening of a sizable surface Dirac gap (82 meV for the doping concentration corresponding to two carbon atoms in the  $3 \times 3$  surface units), which is comparable to that in Fe- or Mn-doped  $\text{Bi}_2\text{Se}_3$  [10,11]. In addition, the Fermi level is drawn back from the bottom of the BCB in the presence of the Se vacancy to near the top of the BVB due to hole doping introduced by  $\text{C}_{\text{Se}}^{4-}$ . The calculated spin texture (Supplemental Material [28]) confirms that the surface Dirac state is not affected by C doping. This indicates that we could open the Dirac gap and tune  $E_f$

in one step [Fig. 1(d)], in contrast to the aforementioned two-step process by magnetic transition metal and charge doping.

In order to understand how a nonmagnetic element such as carbon can open a Dirac gap and tune  $E_f$  simultaneously, we calculated the projected density of states (DOS) of a carbon-doped  $\text{Bi}_2\text{Se}_3$  thin film and present the results in Fig. 2. A strong coupling between the  $2p$  states of the dopant (C) and  $4p/6p$  states of the host (Se/Bi) is clearly seen at the valence band top and conduction band bottom. This  $p$ - $p$  interaction is essentially a result of quantum-mechanical level repulsion, which splits the majority and minority  $2p$  states of carbon and “pushes” the minority  $2p$  states up inside the bulk band gap. The exchange splitting energy between the majority and minority spin  $t_2$  states at the zone center [ $\Delta\epsilon_{\Gamma} = \epsilon(t_2^{\uparrow}) - \epsilon(t_2^{\downarrow})$ ] is substantial ( $\sim 0.80$  eV). Further

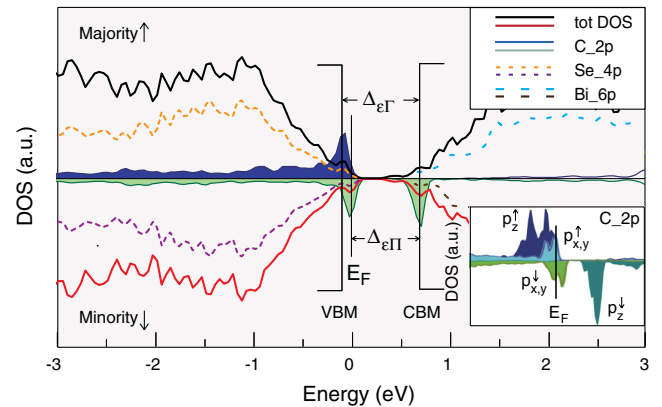


FIG. 2 (color online). Calculated DOS (without SOI) of C-doped  $\text{Bi}_2\text{Se}_3$ . The inset is the projected DOS on carbon  $2p$  orbitals.

examination on the projected  $p$  states of carbon (see the inset in Fig. 2) shows that the  $p_x$  and  $p_y$  orbitals are degenerate. The spin-down  $p_{x,y}$  states are partially occupied, while the spin-down  $p_z$  states are completely empty. The energy difference ( $\Delta\epsilon_{\Pi}$ ) between  $p_{x,y}^{\downarrow}$  and  $p_z^{\downarrow}$  is around 0.66 eV. Such a splitting is due to the change of the carbon bonding environment, especially in the  $z$  direction, under the tetrahedral crystal field. The symmetry and wave function of the impurity state ( $p$ -like  $t_2$ ) are similar to those of the valance band top and conduction band bottom of  $\text{Bi}_2\text{Se}_3$ , which consist mainly of anion Se  $4p$  and cation Bi  $6p$  orbitals [without spin-orbit interaction (SOI)] (Fig. 2) or cation  $6p$  and anion  $4p$  orbitals (with SOI) due to band inversion. Therefore, a strong  $p$ - $p$  coupling between the impurity state and valance band state is allowed near  $E_f$ , resulting in the spin polarization and formation of local moments ( $1.78\mu_B$ ). Such local moments are quite stable, and the spontaneous spin-polarization energy is 175 meV. We considered also the effects of C doping in the middle and bottom (on the side of the vdW gap) Se layers of the first QL and found that the system energetically favors a spin-polarized ground state in both cases, with a magnetic moment of 2.0 and  $1.83\mu_B$ , respectively. This indicates that, even if C substitutes Se at different sites in the first QL, under different experimental conditions, the basic property of the system remains the same. Our calculations also show (see the discussion on the *impurity concentration effect* below) that these local moments favor an out-of-plane long-range ferromagnetic coupling on the surface of  $\text{Bi}_2\text{Se}_3$ , mediated by the surface state. The carbon valence orbitals favor more stable fourfold ( $\Gamma = a_1 + t_2$ ) splitting under the tetrahedral crystal field, forming  $\text{C}^{4-}$  (Fig. 1), which provides two more holes compared to  $\text{Se}^{2-}$ . Therefore,  $\text{C}_{\text{Se}}$  can introduce holes as well as local moments. This duality of carbon doping leads to the simultaneous topological surface state and Fermi level tuning in this intrinsic nonmagnetic topological system.

It is noted that, due to coupling between defect states and surface states, some defect levels appear near the TSS in the bulk gap, similar to that found in transition metal doped TIs [30] and ferromagnetic thin film capped TIs [18]. Interestingly, the carbon impurity states are localized inside the bulk conduction band [Fig. 1(b)] and thus not expected to influence the device performance in a significant way. A band-bending effect has been observed experimentally on the TI surface under the atmospheric environment [4,21,31–34]. Our electrostatic calculations indicate that this effect is not strongly influenced by carbon doping (see the Supplemental Material [28]). Experimentally, the carrier and impurity density are two key parameters. We therefore discuss these effects on the stability and Fermi level tuning in carbon-doped  $\text{Bi}_2\text{Se}_3$ .

*Carrier effect.*—Carriers play critical roles in magnetically doped TIs, in both the bulk and surface. They mediate

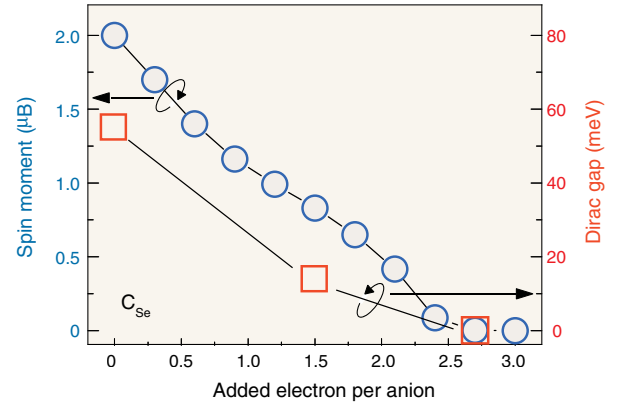


FIG. 3 (color online). Dependence of the spin moment and Dirac gap of C-doped  $\text{Bi}_2\text{Se}_3$  on electron density.

the long-range magnetic order [14] and control  $E_f$  [10,11]. Electrons in the system also affect the localization of magnetic moments, especially in systems with a delocalized  $p$  band and a hole-induced magnetic system. Here, we consider only the effect of electrons on the local moment and Dirac gap in C-doped  $\text{Bi}_2\text{Se}_3$ . In the calculation, excess charges are directly introduced into the system, and a jellium background is used to maintain the charge neutrality of the supercell [27,30]. As shown in Fig. 3, carbon substitutional doping at the anion site induces a magnetic moment of  $\sim 2\mu_B$  per anion. If excess electrons are introduced into the system, which is possible in an experimental environment, they would quench the magnetic moments. Meanwhile, the Dirac gap can be closed if the electron carrier density is sufficiently high.

*Impurity concentration effect.*—The impurity concentration can affect both the degree of localization of magnetic moments and the hole density, because the carbon dopants introduce local moments as well as holes into the system. Figure 4 shows the dependence of the local moment and

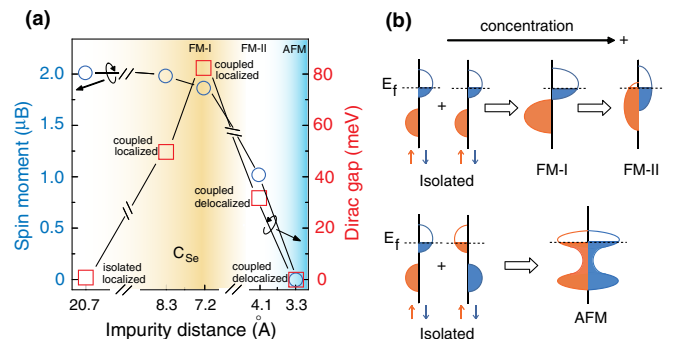


FIG. 4 (color online). (a) Dependence of the magnetic moment and Dirac gap on the interimpurity distance, which is used to indicate the impurity concentration. (b) Schematic illustration of the possible magnetic coupling. The left figure shows the DOS for two isolated carbon dopants, and the right figure shows the coupling when the two carbon dopants are in close proximity at a higher doping concentration.

Dirac gap on the impurity concentration, which is given in terms of distance between impurities, by assuming a uniform dopant distribution. Note that the interimpurity distance in the figure is discontinuous. A high impurity concentration enhances the magnetic coupling and introduces more holes, but too large an impurity concentration would quench the local moment and reduce the size of the Dirac gap. This can be understood based on the phenomenological band-coupling model [35]. Under a very low impurity concentration, the impurity states are localized and isolated, which is insufficient to open a Dirac gap. At a moderate doping concentration, the  $2p$  states with the same spin couple to each other into a ferromagnetic phase (FM phase) but remain localized (FM-I phase), and a Dirac gap opens. The localized impurity bands become broader and delocalized (FM-II phase) as the impurity concentration increases further. This eventually leads to a charge transfer from the majority spin state to the minority spin state, a reduced local moment and exchange splitting (Fig. 4), and a corresponding reduction of the Dirac gap. If the impurity concentration is sufficiently high, the much reduced exchange splitting would lead to an antiferromagnetic phase (AFM phase), even though the energy gain of the FM phase is usually larger than that of the AFM phase in C-doped TI. This is the case when two C dopants are situated in opposite atomic planes, bordering the van der Waals gap, separated by a distance of 3.3 Å. Therefore, a moderate carbon-doping concentration is necessary to open a sizable Dirac gap and to tune the Fermi level close to the Dirac point.

*C-doped TIs vs TM-doped TIs.*—Finally, we wish to make a comment on C-doped TIs and TM-doped TIs. There are several important differences between the C-doped and Fe- or Mn-doped TIs due to the distinctly different orbitals ( $2p$  vs  $3d$ ) of the dopants. First, the  $p$  orbitals of C are usually fully occupied in ionic states, leaving no room for unpaired electrons compared to the  $d$  orbitals of transition metals. Second, the spin-orbit and hyperfine interactions in C are considerably weaker compared to that in TMs, since they scale as the fourth power of the atomic number. Consequently, it is possible to preserve spin coherence over time and distance in C-doped TIs much longer than in TM-doped TIs. Finally, concerning the mechanism of magnetic ordering in TIs, Liu *et al.* proposed a mediation of the long-range ferromagnetism by surface states through the Ruderman-Kittel-Kasuya-Yosida (RKKY) interaction in TM-doped TIs [3,22], while Chang *et al.* suggested the  $p$ - $d$  Van Vleck mechanism (localized  $p$  valence electrons) for the long-range magnetic order [6]. Clearly, the ferromagnetism in carbon-doped  $\text{Bi}_2\text{Se}_3$  challenges our understanding of magnetic ordering, because there are no  $d$  electrons near either conduction or valence bands (Fig. 2). The above  $s$ - $d$  RKKY or  $p$ - $d$  Van Vleck mechanism cannot be applied here. The ferromagnetic double-exchange mechanism can produce large spin

moments, but it is a short-range interaction that requires a mixed valence, i.e.,  $2p^n \leftrightarrow 2p^{n+1}$ . Based on our magnetic calculations, there is no evidence that a mixed valence occurs in C-doped  $\text{Bi}_2\text{Se}_3$ . Therefore, it is reasonable to believe that the spontaneous spin polarization is induced by the  $p$ - $p$  interaction and the magnetic exchange coupling in such a system is mediated by the surface states.

In summary, we propose carbon substitutional doping at Se site as a *one-step* approach to achieve massive TSS in  $\text{Bi}_2\text{Se}_3$ , which is more effective compared to the usual approach of magnetic impurity doping followed by chemical charge doping or vice versa. This is because carbon doping simultaneously introduces localized spin moments and holes. The long-range ordering of the spin moments could be established through  $p$ - $p$  interaction. Meanwhile, holes introduced by carbon doping pull the Fermi level inside the bulk gap from the bulk conduction band. We expect this simple approach of producing massive TSS to promote experimental studies in fabricating C-doped TIs or similar materials and eventually lead to a simpler experimental procedure and robust TIs for broader device applications.

The authors thank Shou-Cheng Zhang, Qi-Kun Xue, Su-Huai Wei, Sergey V. Eremeev, and Lan Wang for their insightful discussions and valuable inputs. This work was collaborated with Yoshiyuki Kawazoe and carried out by using the CCMS SR16000 Supercomputer System at Institute for Materials Research, Tohoku University, funded by the National Research Foundation Singapore under its Competitive Research Program (CRP Grant No. NRFCRP 8-2011-06).

---

\*shenlei@nus.edu.sg

†phyfyp@nus.edu.sg

- [1] M. Z. Hasan and C. L. Kane, *Rev. Mod. Phys.* **82**, 3045 (2010).
- [2] X. L. Qi and S. C. Zhang, *Rev. Mod. Phys.* **83**, 1057 (2011).
- [3] Q. Liu, C. X. Liu, C. Xu, X. L. Qi, and S. C. Zhang, *Phys. Rev. Lett.* **102**, 156603 (2009).
- [4] D. Hsieh, Y. Xia, D. Qian, L. Wray, F. Meier, J. H. Dil, J. Osterwalder, L. Patthey, A. V. Fedorov, H. Lin, A. Bansil, D. Grauer, Y. S. Hor, R. J. Cava, and M. Z. Hasan, *Phys. Rev. Lett.* **103**, 146401 (2009).
- [5] R. Yu, W. Zhang, H. J. Zhang, S. C. Zhang, X. Dai, and Z. Fang, *Science* **329**, 61 (2010).
- [6] C.-Z. Chang, J. Zhang, X. Feng, J. Shen, Z. Zhang, M. Guo, K. Li, Y. Ou, P. Wei, L.-L. Wang, F. Y. Ji, Zhong-Qing, S. Ji, X. Chen, J.-F. Jia, X. Dai, Z. Fang, S.-C. Zhang, K. He, Y. Wang, L. Lu, X.-C. Ma, and Q.-K. Xue, *Science* **340**, 167 (2013).
- [7] X. L. Qi, R. Li, J. Zang, and S. C. Zhang, *Science* **323**, 1184 (2009).
- [8] X. L. Qi, T. L. Hughes, and S. C. Zhang, *Phys. Rev. B* **78**, 195424 (2008).

- [9] J. Wang, X. Chen, B.-F. Zhu, and S.-C. Zhang, *Phys. Rev. B* **85**, 235131 (2012).
- [10] Y.L. Chen, J.H. Chu, J.G. Analytis, Z.K. Liu, K. Igarashi, H.H. Kuo, X.L. Qi, S.K. Mo, R.G. Moore, D.H. Lu, M. Hashimoto, T. Sasagawa, S.C. Zhang, I.R. Fisher, Z. Hussain, and Z.X. Shen, *Science* **329**, 659 (2010).
- [11] L. Wray, S. Xu, Y. Xia, D. Hsieh, A. Fedorov, Y. San Hor, R. Cava, A. Bansil, H. Lin, and M. Hasan, *Nat. Phys.* **7**, 32 (2010).
- [12] Y. Okada, C. Dhital, W. Zhou, E. D. Huemiller, H. Lin, S. Basak, A. Bansil, Y.-B. Huang, H. Ding, Z. Wang, S. D. Wilson, and V. Madhavan, *Phys. Rev. Lett.* **106**, 206805 (2011).
- [13] D. West, Y.Y. Sun, S.B. Zhang, T. Zhang, X. Ma, P. Cheng, Y.Y. Zhang, X. Chen, J.F. Jia, and Q.K. Xue, *Phys. Rev. B* **85**, 081305 (2012).
- [14] Y.S. Hor, P. Roushan, H. Beidenkopf, J. Seo, D. Qu, J.G. Checkelsky, L.A. Wray, D. Hsieh, Y. Xia, S.Y. Xu, D. Qian, M.Z. Hasan, N.P. Ong, A. Yazdani, and R.J. Cava, *Phys. Rev. B* **81**, 195203 (2010).
- [15] J. Henk, A. Ernst, S.V. Eremeev, E.V. Chulkov, I.V. Maznichenko, and I. Mertig, *Phys. Rev. Lett.* **108**, 206801 (2012); J. Henk, M. Flieger, I.V. Maznichenko, I. Mertig, A. Ernst, S.V. Eremeev, and E.V. Chulkov, *Phys. Rev. Lett.* **109**, 076801 (2012).
- [16] M. Liu, J. Zhang, C.-Z. Chang, Z. Zhang, X. Feng, K. Li, K. He, L.-l. Wang, X. Chen, X. Dai, Z. Fang, Q.-K. Xue, X. Ma, and Y. Wang, *Phys. Rev. Lett.* **108**, 036805 (2012).
- [17] M. Ye, S. Eremeev, K. Kuroda, E. Krasovskii, E. Chulkov, Y. Takeda, Y. Saitoh, K. Okamoto, S. Zhu, K. Miyamoto, M. Arita, M. Nakatake, T. Okuda, Y. Ueda, K. Shimada, H. Namatame, M. Taniguchi, and A. Kimura, *Phys. Rev. B* **85**, 205317 (2012).
- [18] S.V. Eremeev, V. Men'shov, V. Tugushev, P. Echenique, and E. Chulkov, *Phys. Rev. B* **88**, 144430 (2013).
- [19] P. Wei, F. Katmis, B.A. Assaf, H. Steinberg, P. Jarillo-Herrero, D. Heiman, and J.S. Moodera, *Phys. Rev. Lett.* **110**, 186807 (2013).
- [20] S.Y. Xu, M. Neupane, C. Liu, D.M. Zhang, A. Richardella, L.A. Wray, N. Alidoust, M. Leandersson, T. Balasubramanian, J. Sánchez-Barriga, O. Rader, G. Landolt, B. Slomski, J.H. Dil, T.-R. Chang, J. Osterwalder, H.-T. Jeng, H. Lin, A. Bansil, N. Samarth, and M.Z. Hasan, [arXiv:1206.2090v3](https://arxiv.org/abs/1206.2090v3).
- [21] M. Koleini, T. Frauenheim, and B. Yan, *Phys. Rev. Lett.* **110**, 016403 (2013).
- [22] D.A. Abanin and D.A. Pesin, *Phys. Rev. Lett.* **106**, 136802 (2011).
- [23] T. Valla, Z.-H. Pan, D. Gardner, Y.S. Lee, and S. Chu, *Phys. Rev. Lett.* **108**, 117601 (2012).
- [24] J. Honolka, A.A. Khajetoorians, V. Sessi, T.O. Wehling, S. Stepanow, J.-L. Mi, B.B. Iversen, T. Schlenk, J. Wiebe, N.B. Brookes, A.I. Lichtenstein, P. Hofmann, K. Kern, and R. Wiesendanger, *Phys. Rev. Lett.* **108**, 256811 (2012).
- [25] M.R. Scholz, J. Sánchez-Barriga, D. Marchenko, A. Varykhalov, A. Volykhov, L. Yashina, and O. Rader, *Phys. Rev. Lett.* **108**, 256810 (2012).
- [26] H. Pan, J.B. Yi, L. Shen, R.Q. Wu, J.H. Yang, J.Y. Lin, Y.P. Feng, J. Ding, L.H. Van, and J.H. Yin, *Phys. Rev. Lett.* **99**, 127201 (2007).
- [27] H.W. Peng, H.J. Xiang, S.-H. Wei, S.-S. Li, J.-B. Xia, and J.B. Li, *Phys. Rev. Lett.* **102**, 017201 (2009).
- [28] See Supplemental Material at <http://link.aps.org/supplemental/10.1103/PhysRevLett.111.236803> for details of the computational method, detailed structural model, band structure of Bi<sub>2</sub>Se<sub>3</sub> with Se vacancies, spin texture, surface band bending, van der Waals' gap, more discussion of the difference between C-doped TIs and C-doped DMSs, and open codes for calculations of parity and spin texture.
- [29] Y. Zhang, K. He, C.Z. Chang, C.L. Song, L.L. Wang, X. Chen, J.F. Jia, Z. Fang, X. Dai, W.Y. Shan, S.Q. Shen, Q. Niu, X.L. Qi, S.C. Zhang, X.C. Ma, and Q.K. Xue, *Nat. Phys.* **6**, 584 (2010).
- [30] C. Niu, Y. Dai, M. Guo, W. Wei, Y. Ma, and B. Huang, *Appl. Phys. Lett.* **98**, 252502 (2011).
- [31] M. Bianchi, R.C. Hatch, J. Mi, B.B. Iversen, and P. Hofmann, *Phys. Rev. Lett.* **107**, 086802 (2011).
- [32] P.D.C. King, R.C. Hatch, M. Bianchi, R. Ovsyannikov, C. Lupulescu, G. Landolt, B. Slomski, J.H. Dil, D. Guan, J.L. Mi, E.D.L. Rienks, J. Fink, A. Lindblad, S. Svensson, S. Bao, G. Balakrishnan, B.B. Iversen, J. Osterwalder, W. Eberhardt, F. Baumberger, and P. Hofmann, *Phys. Rev. Lett.* **107**, 096802 (2011).
- [33] Z.-H. Zhu, G. Levy, B. Ludbrook, C.N. Veenstra, J.A. Rosen, R. Comin, D. Wong, P. Dosanjh, A. Ubaldini, P. Syers, N.P. Butch, J. Paglione, I.S. Elfimov, and A. Damascelli, *Phys. Rev. Lett.* **107**, 186405 (2011).
- [34] M. Bianchi, R.C. Hatch, D. Guan, T. Planke, J. Mi, B.B. Iversen, and P. Hofmann, *Semicond. Sci. Technol.* **27**, 124001 (2012).
- [35] G.M. Dalpian, S.-H. Wei, X.G. Gong, A.J.R. Silva, and A. Fazzio, *Solid State Commun.* **138**, 353 (2006).